PAPER

Check for updates

Application of TMU-17-UR as a pillar-layered MOFs as a hydrogen bonding catalyst for the preparation of pyrazolo[3,4-b]quinolines†

Milad Mohammadi Rasooll,[a] Hassan Sepehrmansourie,*[b] Mohammad Ali Zolfigol, [ID] *[a] Mojtaba Hosseinifard [ID] [c] and Hesam Al-Din Hojjat Shamami[a]

In this report, TMU-17-UR was synthesized as a new H-bond catalyst. In the structure of TMU-17, carboxylic acid and pyridine ligands were used for the formation of desired pillar-layered metal–organic frameworks (MOFs). TMU-17-UR was created *via* a post-modification method by creating urea groups on TMU-17-NH$_2$, which turned it into a suitable H-bond catalyst. The structure of TMU-17-UR was characterized and confirmed using various techniques. The catalytic ability of this structure was investigated in the preparation of pyrazolo[3,4-b]quinolines as important biological compounds under environmentally friendly and mild reaction conditions. The structure of the obtained products was confirmed using techniques such as FT-IR, ^{1}H-NMR, ^{13}C-NMR and their melting point. The results obtained here have shown that the development of task-specific heterogeneous catalysts can be continued.

Introduction

Pillar-layered MOFs are an important class of MOFs that received attention recently. Pillar-layered MOFs in their structure have alternating layers with columns containing metal and organic ligands.[1–3] The pillars and ligands in their framework are held together by coordination bonds and form a three-dimensional porous structure with suitable surface area and adjustable pore size. Pillar-layered MOFs have considerable versatility, as they can be synthesized from different metals such as copper, zinc, or cobalt. Also, various organic ligands can be used in their structure, which gives various chemical properties to this type of MOFs.[4,5] Due to the diversity of their structure, these three-dimensional compounds have various applications in various fields, such as gas storage, catalysts, drug delivery, *etc.*.[6–8] One of the characteristics of pillar-layered MOFs is that the structure of these compounds can be easily changed by replacing the metal column or organic ligand components, increasing their functional diversity.[9]

Urea derivatives are one of the most important studied organic structures in the field of catalysts. Urea derivatives have been used as catalysts in many organic reactions such as Strecker, Mannich, Friedel–Crafts reactions, *etc.* The hydrogen bonding agent activates the substrate for catalysis through donor/acceptor acidic N–H bonds and nitrogen lone pairs.[10–14] Combining H-bond catalysts with MOFs can lead to the development of new heterogeneous catalysts with higher activity and selectivity. In this case, metal–organic frameworks are designed that will have the ability to give hydrogen bonding, which has been considered in recent studies.[15–18] It is worth noting that the porous nature of MOFs allows the diffusion of reactive molecules in the catalyst sites, which can increase the reaction efficiency.[19,20] Metal–organic frameworks, which have shown their importance as a new generation of nanoreactors in recent years, can act as a suitable bed with pendants such as urea or thiourea groups as hydrogen bonding donors.[21,22] H-bond donating MOF catalysts are new-generation catalysts that can play a role as catalysts for the production of pharmaceutical products and organic compounds.[23,24] These MOFs have good properties such as high chemical and thermal stability as well as good activity. The selectivity of this type of hydrogen bond catalyst is high, which in turn can be effective in increasing product yield and saving energy.[25,26]

In recent years, the importance of new and effective medicinal compounds has increased. Various research studies have been conducted in this field, which has been accompanied by significant progress.[27,28] It should be considered that these compounds need to be expanded. Heterocyclic compounds have suitable medicinal properties and have been used in various fields, such as antidepressants, antifungals, antimalarials, anticancer, *etc.*.[29,30] Also, these compounds have been used

aDepartment of Organic Chemistry, Faculty of Chemistry, Faculty of Chemistry and Petroleum Sciences, Bu-Ali Sina University, Hamedan 6517838683, Iran. E-mail: zolfi@basu.ac.ir; mzolfigol@yahoo.com; Fax: +988138380709; Tel: +988138282807
bFaculty of Converging Science and Technologies, University of Qom, Qom, 37185-359, Iran. E-mail: sepehr9129@yahoo.com
cDepartment of Energy, Materials and Energy Research Center, Karaj 401602, Iran
† Electronic supplementary information (ESI) available. See DOI: https://doi.org/10.1039/d5ra01752a
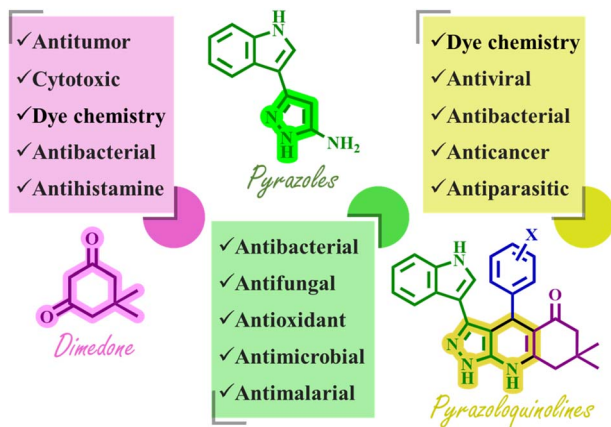
Fig. 1 Various properties of dimedone, pyrazole and pyrazoloquinoline compounds.

in various industries such as agriculture and paint production. Heterocyclic compounds are formed from important nuclei. Among the most important effective nuclei, we can mention pyrazoles, pyrazoloquinoline, dimedone, *etc.*, which give suitable properties to the synthesized compound. Fig. 1 shows the most important properties of these cores that have been proven.[31–36] Pyrazolo[3,4-*b*]quinoline compounds have shown important biological activities including anti-inflammatory, anti-cancer and antimicrobial properties. Also, the unique biological properties of these compounds have been confirmed in the treatment of many neurological diseases.[37–39]

In continuation of the research on targeted catalysts, the design of the catalyst based on the metal–organic framework is the main goal of this research. In this report, a pillar-layered MOFs containing acidic and pyridine ligands is used, and in the next step, urea group is created on it by solvothermal method. This method creates an efficient hydrogen bonding catalyst based on metal–organic frameworks. The use of this catalyst in the preparation of pyrazolo[3,4-*b*]quinoline derivatives will be investigated to determine the importance of the design of this catalyst. The created pyrazolo[3,4-*b*]quinoline derivatives have effective medicinal cores. These derivatives are

synthesized in solvent-free conditions with a mild and green method.

Experimental section

Preparation of TMU-17-NH$_2$

The preparation of TMU-17-NH$_2$ was done through the solvothermal method according to the method of the previous report.[40] Initially, NH$_2$-BDC (1 mmol, 0.181 g), Zn(NO$_3$)$_2$·6H$_2$O (1 mmol, 0.298 g), and 1,4-bis(4-pyridyl)-2,3-diaza-2,3-butadiene (4-bpdb) (1 mmol, 0.210 g) were dissolved in 15 mL of DMF. The resulting mixture was transferred to a 60 mL Teflon autoclave and heated at 80 °C for 3 days. After this time, the autoclave was allowed to cool down to room temperature, and the product was formed. The crystals obtained were separated from the soluble compounds by centrifugation (2 × 4000 rpm). Finally, the obtained TMU-17-NH$_2$ crystals were washed with ethanol (EtOH) and DMF (2 × 10 mL). In the last step, it was immersed in CHCl$_3$ for 24 h and dried in a vacuum oven at 100 °C for 24 h.

Preparation of TMU-17-UR as an H-bond pillar-layered MOFs-based catalyst

The solvothermal method was used for the synthesis of TMU-17-NH$_2$ and its functionalization through post-modification. A mixture of phenyl isocyanate (5 mmol, 0.595 g), TMU-17-NH$_2$ (0.2 g), and dry CH$_3$CN (10 mL) as a solvent was stirred for 30 min at 25 °C. Then the reaction mixture was placed in a 25 mL Teflon autoclave and heated at 120 °C for 12 h. Then the precipitate obtained was separated using a centrifuge (2 × 4000 rpm min^{-1}) and washed with CH$_3$CN and EtOH 3 times. Finally, TMU-17-UR was dried at 80 °C for 12 h (Scheme 1).

Catalytic reaction

For the preparation of pyrazolo[3,4-*b*]quinoline derivatives, in a 10 mL round-bottomed flask, a mixture of aromatic aldehydes (0.5 mmol), dimedone (0.5 mmol, 0.07 g), 3-(1*H*-indol-3-yl)-1*H*-pyrazol-5-amine and 3-(4-chlorophenyl)-1*H*-pyrazol-5-amine (0.5 mmol), which has been synthesized according to previous reports[41,42] and TMU-17-UR as an H-bond pillar-layered MOFs-based catalyst (15 mg) were stirred at 100 °C. After the
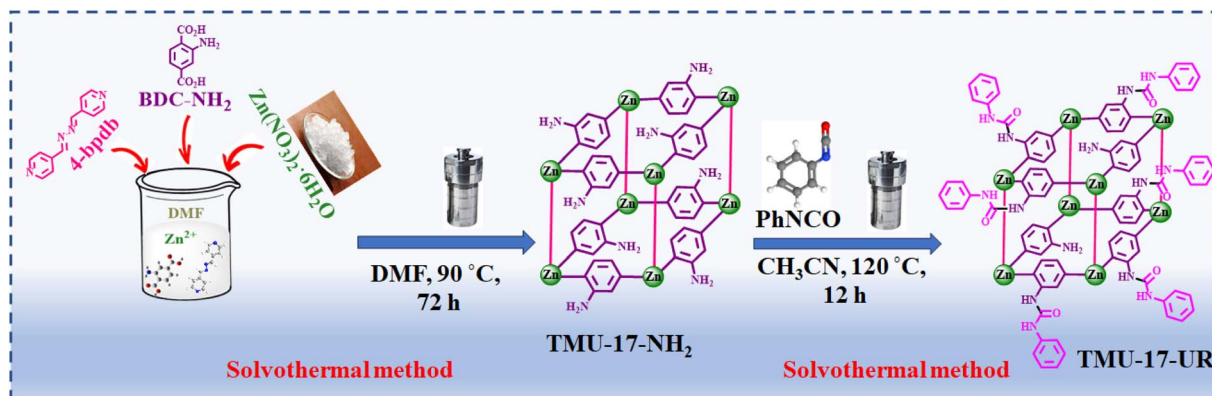
Scheme 1 Schematic general strategy for preparation of TMU-17-UR as an efficient H-bond pillar-layered MOFs-based catalyst.
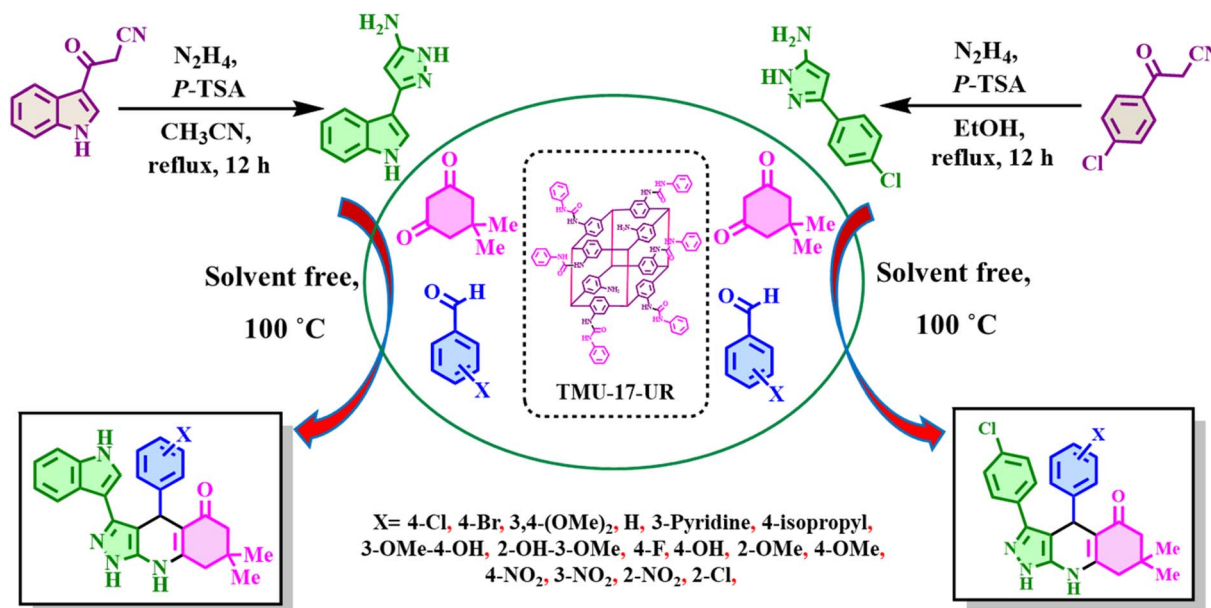
Scheme 2 Synthesis of pyrazolo[3,4-b]quinoline derivatives using TMU-17-UR as an efficient H-bond pillar-layered MOFs-based catalyst.

completion of the reaction that was monitored by the TLC technique, the catalyst was isolated from the reaction mixture by centrifugation (2×4000 rpm min^{-1}) after adding hot ethanol (20 mL). After, the solvent evaporates to form a precipitate. Finally, in order to purify the synthesized products, the resulting precipitate was washed several times with cold EtOH. The pyrazolo[3,4-b]quinoline derivatives were obtained in high yield (70–85%) (Scheme 2).

Spectral data of pyrazolo[3,4-b]quinoline derivatives

4-(4-Chlorophenyl)-3-(1H-indol-3-yl)-7,7-dimethyl-1,4,6,7,8,9-hexahydro-5H-pyrazolo[3,4-b]quinolin-5-one (FC1). Yellow solid; Mp: >300 °C; FT-IR (KBr, cm^{-1}): 3406, 3253, 3167, 1657, 1614. ^{1}H NMR (250 MHz, DMSO-d_6) δ_{ppm} 12.17 (s, 1H), 11.33 (s, 1H), 9.91 (s, 1H), 7.63 (d, $J = 7.2$ Hz, 1H), 7.38 (d, $J = 7.5$ Hz, 1H), 7.21 (s, 1H), 7.12–6.93 (m, 6H), 5.19 (s, 1H), 2.45–2.27 (m, 2H), 2.13 (d, $J = 16.1$ Hz, 1H), 1.93 (d, $J = 16.1$ Hz, 1H), 0.98 (s, 3H), 0.84 (s, 3H). ^{13}C NMR (63 MHz, DMSO-d_6) δ_{ppm} 193.2, 153.0, 147.4, 136.3, 134.7, 130.0, 129.6, 127.8, 125.2, 124.8, 122.2, 120.0, 112.2, 107.7, 105.0, 102.5, 50.9, 41.4, 35.2, 32.4, 29.3, 27.1.

4-(4-Chlorophenyl)-3-(1H-indol-3-yl)-7,7-dimethyl-1,4,6,7,8,9-hexahydro-5H-pyrazolo[3,4-b]quinolin-5-one (FC1) (D$_2$O exchange). ^{1}H NMR (250 MHz, DMSO-d_6) δ_{ppm} 7.58 (d, $J = 7.4$ Hz, 1H), 7.39 (d, $J = 7.7$ Hz, 1H), 7.22 (s, 1H), 7.09–6.92 (m, 6H), 5.17 (s, 1H), 2.42 (d, $J = 9.3$ Hz, 2H), 2.13 (d, $J = 16.3$ Hz, 1H), 1.92 (d, $J = 16.1$ Hz, 1H), 0.96 (s, 3H), 0.81 (s, 3H).

4-(4-Bromophenyl)-3-(1H-indol-3-yl)-7,7-dimethyl-1,4,6,7,8,9-hexahydro-5H-pyrazolo[3,4-b]quinolin-5-one (FC2). Yellow solid; Mp: >300 °C; FT-IR (KBr, cm^{-1}): 3320, 3248, 3158, 1655, 1501. ^{1}H NMR (400 MHz, DMSO-d_6) δ_{ppm} 12.20 (s, 1H), 11.38 (s, 1H), 9.94 (s, 1H), 7.65 (d, $J = 7.9$ Hz, 1H), 7.41 (d, $J = 8.1$ Hz, 1H), 7.25 (d, $J = 2.7$ Hz, 2H), 7.23 (s, 1H), 7.15 (t, $J =$

7.4 Hz, 1H), 7.07 (t, $J = 7.4$ Hz, 1H), 6.96 (d, $J = 8.4$ Hz, 2H), 5.21 (s, 1H), 2.50 (d, $J = 8.0$ Hz, 1H), 2.40 (d, $J = 16.6$ Hz, 1H), 2.16 (d, $J = 16.0$ Hz, 1H), 1.97 (d, $J = 16.0$ Hz, 1H), 1.02 (s, 3H), 0.88 (s, 3H). ^{13}C NMR (101 MHz, DMSO-d_6) δ_{ppm} 192.7, 162.3, 152.5, 147.4, 147.3, 135.8, 134.2, 130.3, 129.5, 124.7, 124.3, 121.7, 119.5, 119.4, 118.1, 111.8, 107.1, 104.4, 102.0, 50.4, 40.9, 34.8, 31.9, 28.9, 26.7.

4-(3,4-Dimethoxyphenyl)-3-(1H-indol-3-yl)-7,7-dimethyl-1,4,6,7,8,9-hexahydro-5H-pyrazolo[3,4-b]quinolin-5-one (FC3). Yellow solid; Mp: >300 °C; FT-IR (KBr, cm^{-1}): 3249, 3060, 2964, 1561, 1500. ^{1}H NMR (250 MHz, DMSO-d_6) δ_{ppm} 12.08 (s, 1H), 11.37 (s, 1H), 9.78 (s, 1H), 7.64 (d, $J = 5.9$ Hz, 1H), 7.40 (d, $J = 7.2$ Hz, 1H), 7.29 (s, 1H), 7.17–7.04 (m, 2H), 6.59 (d, $J = 8.0$ Hz, 1H), 6.50–6.38 (m, 2H), 5.16 (s, 1H), 3.55 (s, 3H), 3.25 (s, 3H), 2.77 (d, $J = 38.6$ Hz, 1H), 2.39 (d, $J = 17.6$ Hz, 1H), 2.15 (d, $J = 15.9$ Hz, 1H), 1.97 (d, $J = 16.0$ Hz, 1H), 1.01 (s, 3H), 0.93 (s, 3H). ^{13}C NMR (63 MHz, DMSO-d_6) δ_{ppm} 193.3, 153.0, 148.0, 147.6, 146.7, 141.3, 136.4, 134.4, 125.4, 125.0, 122.1, 120.0, 118.9, 112.2, 111.9, 111.7, 107.8, 105.3, 103.5, 55.7, 55.1, 51.0, 41.4, 35.0, 32.3, 29.5, 27.2.

3-(1H-Indol-3-yl)-7,7-dimethyl-4-phenyl-1,4,6,7,8,9-hexahydro-5H-pyrazolo[3,4-b]quinolin-5-one (FC4). Yellow solid; Mp: >300 °C; FT-IR (KBr, cm^{-1}): 3268, 3202, 3050, 1633, 1614. ^{1}H NMR (400 MHz, DMSO-d_6) δ_{ppm} 12.19 (s, 1H), 11.37 (s, 1H), 9.89 (s, 1H), 7.68 (d, $J = 7.9$ Hz, 1H), 7.41 (d, $J = 8.1$ Hz, 1H), 7.21 (d, $J = 2.4$ Hz, 1H), 7.15 (t, $J = 7.2$ Hz, 1H), 7.09–7.05 (m, 2H), 7.05–7.02 (m, 3H), 6.98–6.93 (m, 1H), 5.21 (s, 1H), 2.50–2.37 (m, 2H), 2.16 (d, $J = 16.0$ Hz, 1H), 1.97 (d, $J = 16.0$ Hz, 1H), 1.02 (s, 3H), 0.88 (s, 3H). ^{13}C NMR (101 MHz, DMSO-d_6) δ_{ppm} 192.7, 162.3, 152.4, 148.1, 135.8, 128.1, 127.5, 127.3, 125.1, 124.8, 124.2, 121.6, 119.6, 119.5, 111.7, 107.7, 102.6, 50.5, 41.0, 35.1, 31.9, 28.9, 26.6.

3-(1H-Indol-3-yl)-7,7-dimethyl-4-(pyridin-3-yl)-1,4,6,7,8,9-hexahydro-5H-pyrazolo[3,4-b]quinolin-5-one (FC5). Yellow

solid; Mp: >300 °C; FT-IR (KBr, cm^{-1}): 3241, 2955, 1614, 1594, 1561. ^{1}H NMR (400 MHz, DMSO-d_6) δ_{ppm} 12.23 (s, 1H), 11.39 (s, 1H), 10.00 (s, 1H), 8.20 (s, 1H), 8.11 (dd, J = 4.7, 1.5 Hz, 1H), 7.64 (d, J = 7.9 Hz, 1H), 7.41 (d, J = 8.1 Hz, 1H), 7.33 (d, J = 2.5 Hz, 1H), 7.29 (d, J = 7.8 Hz, 1H), 7.15 (t, J = 7.3 Hz, 1H), 7.09–7.04 (m, 2H), 5.26 (s, 1H), 2.53 (d, J = 13.7 Hz, 1H), 2.44 (d, J = 16.6 Hz, 1H), 2.17 (d, J = 16.0 Hz, 1H), 1.98 (d, J = 16.0 Hz, 1H), 1.03 (s, 3H), 0.89 (s, 3H). ^{13}C NMR (101 MHz, DMSO-d_6) δ_{ppm} 192.7, 152.9, 148.5, 147.1, 146.3, 143.0, 135.8, 134.4, 134.3, 124.8, 124.4, 123.0, 121.7, 119.5, 119.4, 111.8, 106.6, 104.2, 101.8, 50.3, 40.9, 33.1, 31.9, 28.8, 26.7.

3-(1H-Indol-3-yl)-4-(4-isopropylphenyl)-7,7-dimethyl-1,4,6,7,8,9-hexahydro-5H-pyrazolo[3,4-b]quinolin-5-one (FC6). Yellow solid; Mp: >300 °C; FT-IR (KBr, cm^{-1}): 3347, 3274, 3055, 1675,1627, 1609. ^{1}H NMR (400 MHz, DMSO-d_6) δ_{ppm} 12.13 (s, 1H), 11.38 (s, 1H), 9.84 (s, 1H), 7.67 (d, J = 7.9 Hz, 1H), 7.41 (d, J = 8.1 Hz, 1H), 7.24 (d, J = 2.4 Hz, 1H), 7.15 (t, J = 7.4 Hz, 1H), 7.06 (t, J = 7.4 Hz, 1H), 6.97–6.88 (m, 4H), 5.18 (s, 1H), 2.72 (p, 1H), 2.49–2.39 (m, 2H), 2.15 (d, J = 16.0 Hz, 1H), 1.99 (d, J = 16.0 Hz, 1H), 1.09 (s, 3H), 1.08 (s, 3H), 1.02 (s, 3H), 0.91 (s, 3H). ^{13}C NMR (101 MHz, DMSO-d_6) δ_{ppm} 192.7, 152.5, 147.5, 145.6, 144.9, 135.8, 133.8, 128.1, 127.1, 125.4, 124.7, 124.2, 121.7, 119.6, 119.5, 111.7, 107.8, 104.7, 102.8, 50.5, 41.0, 32.8, 31.9, 28.8, 26.9, 23.9, 23.7.

4-(4-Hydroxy-3-methoxyphenyl)-3-(1H-indol-3-yl)-7,7-dimethyl-1,4,6,7,8,9-hexahydro-5H-pyrazolo[3,4-b]quinolin-5-one (FC7). Yellow solid; Mp: >300 °C; FT-IR (KBr, cm^{-1}): 3253, 3162, 3068, 1658, 1599. ^{1}H NMR (400 MHz, DMSO-d_6) δ_{ppm} 12.10 (s, 1H), 11.40 (s, 1H), 9.79 (s, 1H), 8.46 (s, 1H), 7.67 (d, J = 7.9 Hz, 1H), 7.43 (d, J = 8.1 Hz, 1H), 7.30 (d, J = 2.5 Hz, 1H), 7.17 (t, J = 7.5 Hz, 1H), 7.10 (t, J = 7.4 Hz, 1H), 6.49–6.43 (m, 2H), 6.33 (d, J = 8.1 Hz, 1H), 5.14 (s, 1H), 3.32 (s, 3H), 2.50–2.39 (m, 2H), 2.17 (d, J = 16.0 Hz, 1H), 2.00 (d, J = 15.9 Hz, 1H), 1.04 (s, 3H), 0.96 (s, 3H). ^{13}C NMR (101 MHz, DMSO-d_6) δ_{ppm} 192.8, 162.3, 152.4, 147.2, 146.4, 143.8, 139.4, 135.9, 133.8, 124.9, 124.5, 121.6, 119.5, 118.9, 114.7, 111.7, 107.6, 104.9, 103.2, 54.9, 50.6, 41.0, 34.4, 31.9, 29.0, 26.8.

4-(2-Hydroxy-3-methoxyphenyl)-3-(1H-indol-3-yl)-7,7-dimethyl-1,4,6,7,8,9-hexahydro-5H-pyrazolo[3,4-b]quinolin-5-one (FC8). Yellow solid; Mp: >300 °C; FT-IR (KBr, cm^{-1}): 3308, 3213, 3054, 1670, 1611. ^{1}H NMR (400 MHz, DMSO-d_6) δ_{ppm} 12.38 (s, 1H), 11.50 (s, 1H), 10.52 (s, 1H), 10.08 (s, 1H), 7.86 (d, J = 7.9 Hz, 1H), 7.39 (d, J = 8.1 Hz, 1H), 7.18 (t, J = 7.5 Hz, 1H), 7.10 (t, J = 7.4 Hz, 1H), 6.88 (d, J = 2.1 Hz, 1H), 6.70–6.65 (m, 2H), 6.38 (dd, J = 7.2, 2.1 Hz, 1H), 5.31 (s, 1H), 3.77 (s, 3H), 2.55–2.46 (m, 2H), 2.33 (d, J = 16.5 Hz, 1H), 2.17 (d, J = 16.4 Hz, 1H), 1.07 (s, 3H), 0.89 (s, 3H). ^{13}C NMR (101 MHz, DMSO-d_6) δ_{ppm} 195.5, 156.0, 149.0, 147.4, 142.3, 136.0, 135.7, 134.1, 124.1, 123.7, 121.8, 120.6, 119.9, 119.6, 111.6, 109.6, 107.3, 104.5, 102.1, 55.3, 49.5, 41.1, 32.0, 28.5, 28.3, 26.6.

4-(4-Fluorophenyl)-3-(1H-indol-3-yl)-7,7-dimethyl-1,4,6,7,8,9-hexahydro-5H-pyrazolo[3,4-b]quinolin-5-one (FC9). Yellow solid; Mp: >300 °C; FT-IR (KBr, cm^{-1}): 3250, 2956, 1657, 1600, 1564. ^{1}H NMR (400 MHz, DMSO-d_6) δ_{ppm} 12.19 (s, 1H), 11.37 (s, 1H), 9.92 (s, 1H), 7.66 (d, J = 7.8 Hz, 1H), 7.41 (d, J = 8.1 Hz, 1H), 7.23 (d, J = 2.3 Hz, 1H), 7.15 (t, J = 7.5 Hz, 1H), 7.08 (d, J = 7.4 Hz, 1H), 7.05–7.01 (m, 2H), 6.87 (t, J = 8.8 Hz, 2H), 5.23 (s, 1H), 2.50–2.36 (m, 2H), 2.16 (d, J = 16.0 Hz, 1H), 1.98 (d, J = 16.0 Hz, 1H), 1.02 (s, 3H), 0.88 (s, 3H). ^{13}C NMR (101 MHz, DMSO-d_6) δ_{ppm} 192.7, 162.3, 161.1, 158.7, 152.4, 147.3, 144.2, 135.8, 134.1, 128.9, 128.8, 124.7, 124.3, 121.7, 119.5, 114.2, 111.8, 107.5, 104.5, 102.4, 50.4, 40.9, 34.5, 31.9, 28.9, 26.6.

4-(4-Hydroxyphenyl)-3-(1H-indol-3-yl)-7,7-dimethyl-1,4,6,7,8,9-hexahydro-5H-pyrazolo[3,4-b]quinolin-5-one (FC10). Yellow solid; Mp: >300 °C; FT-IR (KBr, cm^{-1}): 3275, 3165, 2956, 1594, 1553. ^{1}H NMR (400 MHz, DMSO-d_6) δ_{ppm} 12.11 (s, 1H), 11.35 (s, 1H), 9.79 (s, 1H), 8.95 (s, 1H), 7.70 (d, J = 7.8 Hz, 1H), 7.41 (d, J = 8.1 Hz, 1H), 7.18 (d, J = 2.4 Hz, 1H), 7.14 (d, J = 7.6 Hz, 1H), 7.07 (t, J = 7.4 Hz, 1H), 6.84 (d, J = 8.2 Hz, 2H), 6.46 (d, J = 8.4 Hz, 2H), 5.09 (s, 1H), 2.46–2.35 (m, 2H), 2.14 (d, J = 16.0 Hz, 1H), 1.96 (d, J = 16.0 Hz, 1H), 1.02 (s, 3H), 0.88 (s, 3H). ^{13}C NMR (101 MHz, DMSO-d_6) δ_{ppm} 192.7, 154.7, 152.0, 147.5, 138.8, 135.8, 133.8, 128.2, 124.7, 124.2, 121.7, 119.5, 114.2, 111.7, 108.2, 104.7, 102.9, 50.5, 40.9, 34.1, 31.9, 28.9, 26.6.

3-(4-Chlorophenyl)-4-(2-methoxyphenyl)-7,7-dimethyl-1,4,6,7,8,9-hexahydro-5H-pyrazolo[3,4-b]quinolin-5-one (FD1). Yellow solid; Mp: >300 °C; FT-IR (KBr, cm^{-1}): 3254, 3126, 1662, 1627, 1583. ^{1}H NMR (400 MHz, DMSO-d_6) δ_{ppm} 12.44 (s, 1H), 9.86 (s, 1H), 7.57 (d, J = 8.6 Hz, 2H), 7.46 (d, J = 8.6 Hz, 2H), 7.04 (dd, J = 7.5, 1.6 Hz, 1H), 6.97–6.92 (m, 1H), 6.73 (d, J = 7.7 Hz, 1H), 6.69 (t, J = 7.4 Hz, 1H), 5.61 (s, 1H), 3.61 (s, 3H), 2.49 (s, 1H), 2.38 (d, J = 16.4 Hz, 1H), 2.13 (d, J = 16.0 Hz, 1H), 1.90 (d, J = 15.9 Hz, 1H), 1.02 (s, 3H), 0.89 (s, 3H). ^{13}C NMR (101 MHz, DMSO-d_6) δ_{ppm} 192.3, 155.4, 152.5, 148.3, 136.1, 135.8, 132.2, 129.5, 128.4, 128.3, 128.1, 126.6, 119.8, 110.7, 107.4, 104.0, 55.0, 50.5, 40.9, 31.9, 29.4, 29.1, 26.4.

3-(4-Chlorophenyl)-4-(4-methoxyphenyl)-7,7-dimethyl-1,4,6,7,8,9-hexahydro-5H-pyrazolo[3,4-b]quinolin-5-one (FD2). Yellow solid; Mp: >300 °C; FT-IR (KBr, cm^{-1}): 3179, 2956, 1583, 1561, 1539. ^{1}H NMR (250 MHz, DMSO-d_6) δ_{ppm} 12.60 (s, 1H), 9.87 (s, 1H), 7.53 (d, J = 5.8 Hz, 2H), 7.43 (d, J = 7.8 Hz, 2H), 6.99 (d, J = 7.9 Hz, 2H), 6.62 (d, J = 8.1 Hz, 2H), 5.25 (s, 1H), 3.58 (s, 3H), 2.45–2.27 (m, 2H), 2.12 (d, J = 16.1 Hz, 1H), 1.92 (d, J = 15.8 Hz, 1H), 0.97 (s, 3H), 0.81 (s, 3H). ^{13}C NMR (63 MHz, DMSO-d_6) δ_{ppm} 193.3, 157.4, 152.3, 148.6, 140.1, 136.5, 132.8, 129.2, 128.8, 128.3, 128.0, 113.4, 108.4, 104.4, 55.2, 50.8, 41.3, 34.7, 32.3, 29.4, 27.0.

3-(4-Chlorophenyl)-4-(4-methoxyphenyl)-7,7-dimethyl-1,4,6,7,8,9-hexahydro-5H-pyrazolo[3,4-b]quinolin-5-one (FD2) (D$_2$O exchange). ^{1}H NMR (250 MHz, DMSO-d_6) δ_{ppm} 7.46 (d, J = 8.2 Hz, 2H), 7.36 (d, J = 7.4 Hz, 2H), 6.95 (d, J = 8.0 Hz, 2H), 6.57 (d, J = 7.7 Hz, 2H), 5.21 (s, 1H), 3.52 (s, 3H), 2.45–2.26 (m, 2H), 2.12 (d, J = 16.4 Hz, 1H), 1.91 (d, J = 16.3 Hz, 1H), 0.93 (s, 3H), 0.78 (s, 3H).

3-(4-Chlorophenyl)-7,7-dimethyl-4-(4-nitrophenyl)-1,4,6,7,8,9-hexahydro-5H-pyrazolo[3,4-b]quinolin-5-one (FD3). Yellow solid; Mp: >300 °C; FT-IR (KBr, cm^{-1}): 3415, 3276, 2951, 1514, 1350. ^{1}H NMR (400 MHz, DMSO-d_6) δ_{ppm} 12.76 (s, 1H), 10.15 (s, 1H), 8.00 (s, 1H), 7.97 (d, J = 6.3 Hz, 1H), 7.55 (d, J = 8.6 Hz, 2H), 7.46 (d, J = 8.6 Hz, 2H), 7.37 (d, J = 8.8 Hz, 2H), 5.50 (s, 1H), 2.55 (s, 1H), 2.41 (d, J = 16.5 Hz, 1H), 2.17 (d, J = 16.1 Hz, 1H), 1.96 (d, J = 16.0 Hz, 1H), 1.02 (s, 3H), 0.85 (s, 3H).

3-(4-Chlorophenyl)-7,7-dimethyl-4-(3-nitrophenyl)-1,4,6,7,8,9-hexahydro-5H-pyrazolo[3,4-b]quinolin-5-one (FD4). Yellow solid; Mp: >300 °C; FT-IR (KBr, cm^{-1}): 3251, 3185, 1627, 1530, 1350. ^{1}H NMR (400 MHz, DMSO-d_6) δ_{ppm} 12.76 (s, 1H), 10.15 (s, 1H), 7.92 (s, 1H), 7.85 (d, J = 8.1 Hz, 1H), 7.60–7.52 (m, 3H), 7.45 (d, J = 8.4 Hz, 2H), 7.39 (t, J = 7.9 Hz, 1H), 5.53 (s, 1H), 2.55 (s, 1H), 2.43 (d, J = 16.6 Hz, 1H), 2.18 (d, J = 16.1 Hz, 1H), 1.98 (d, J = 16.1 Hz, 1H), 1.02 (s, 3H), 0.86 (s, 3H). ^{13}C NMR (101 MHz, DMSO-d_6) δ_{ppm} 192.8, 152.7, 149.3, 147.2, 134.1, 132.7, 129.1, 128.7, 127.9, 121.8, 120.6, 106.5, 102.5, 50.2, 40.8, 35.3, 32.0, 28.8, 26.5.

4-(2-Chlorophenyl)-3-(4-chlorophenyl)-7,7-dimethyl-1,4,6,7,8,9-hexahydro-5H-pyrazolo[3,4-b]quinolin-5-one (FD5). Yellow solid; Mp: >300 °C; FT-IR (KBr, cm^{-1}): 3202, 3047, 1625, 1577, 1561. ^{1}H NMR (400 MHz, DMSO-d_6) δ_{ppm} 12.54 (s, 1H), 10.03 (s, 1H), 7.45 (d, J = 8.7 Hz, 2H), 7.41 (d, J = 8.6 Hz, 2H), 7.23 (d, J = 7.3 Hz, 1H), 7.12–7.05 (m, 2H), 6.97 (td, J = 7.7, 1.5 Hz, 1H), 5.62 (s, 1H), 2.50–2.32 (m, 2H), 2.14 (d, J = 16.1 Hz, 1H), 1.92 (d, J = 16.0 Hz, 1H), 1.02 (s, 3H), 0.90 (s, 3H). ^{13}C NMR (101 MHz, DMSO-d_6) δ_{ppm} 192.5, 152.6, 147.8, 144.2, 137.2, 132.6, 131.7, 131.5, 129.1, 128.7, 128.3, 128.2, 127.0, 126.3, 106.6, 102.7, 50.4, 40.9, 33.9, 31.8, 28.9, 26.5.

3-(4-Chlorophenyl)-7,7-dimethyl-4-(2-nitrophenyl)-1,4,6,7,8,9-hexahydro-5H-pyrazolo[3,4-b]quinolin-5-one (FD6). Yellow solid; Mp: >300 °C; FT-IR (KBr, cm^{-1}): 3246, 3187, 1584, 1531, 1357. ^{1}H NMR (400 MHz, DMSO-d_6) δ_{ppm} 12.76 (s, 1H), 10.15 (s, 1H), 7.69–7.65 (m, 1H), 7.51 (d, J = 8.5 Hz, 2H), 7.47 (d, J = 7.3 Hz, 1H), 7.37 (d, J = 8.6 Hz, 2H), 7.26–7.21 (m, 1H), 7.18–7.14 (m, 1H), 6.06 (s, 1H), 2.46–2.29 (m, 2H), 2.07 (d, J = 16.1 Hz, 1H), 1.86 (d, J = 16.3 Hz, 1H), 0.97 (s, 3H), 0.74 (s, 3H). ^{13}C NMR (101 MHz, DMSO-d_6) δ_{ppm} 192.7, 152.1, 148.3, 147.9, 141.2, 137.4, 132.8, 132.7, 131.2, 130.9, 128.4, 128.4, 126.6, 123.3, 107.0, 101.8, 50.0, 40.8, 31.9, 30.3, 28.6, 26.3.

3-(4-Chlorophenyl)-7,7-dimethyl-4-(pyridin-3-yl)-1,4,6,7,8,9-hexahydro-5H-pyrazolo[3,4-b]quinolin-5-one (FD7). Yellow solid; Mp: >300 °C; FT-IR (KBr, cm^{-1}): 3427, 3170, 1619, 1584, 1538. ^{1}H NMR (400 MHz, DMSO-d_6) δ_{ppm} 12.72 (s, 1H), 10.08 (s, 1H), 8.35 (s, 1H), 8.16 (d, J = 3.5 Hz, 1H), 7.56 (d, J = 8.5 Hz, 2H), 7.48 (d, J = 8.5 Hz, 2H), 7.40 (d, J = 7.9 Hz, 1H), 7.12 (dd, J = 7.8, 4.8 Hz, 1H), 5.38 (s, 1H), 2.50–2.37 (m, 2H), 2.17 (d, J = 16.1 Hz, 1H), 1.97 (d, J = 16.0 Hz, 1H), 1.02 (s, 3H), 0.86 (s, 3H). ^{13}C NMR (101 MHz, DMSO-d_6) δ_{ppm} 192.7, 152.5, 148.6, 147.8, 146.6, 142.4, 136.5, 134.66, 132.5, 130.9, 129.3, 128.8, 127.7, 123.1, 106.7, 102.8, 50.3, 40.8, 33.2, 31.9, 28.8, 26.5.

3-(4-Chlorophenyl)-4-(3,4-dimethoxyphenyl)-7,7-dimethyl-1,4,6,7,8,9-hexahydro-5H-pyrazolo[3,4-b]quinolin-5-one (FD8). Yellow solid; Mp: >300 °C; FT-IR (KBr, cm^{-1}): 3267, 3195, 1585, 1506, 1420. ^{1}H NMR (400 MHz, DMSO-d_6) δ_{ppm} 12.61 (s, 1H), 9.91 (s, 1H), 7.60 (d, J = 8.6 Hz, 2H), 7.50 (d, J = 8.6 Hz, 2H), 6.74 (d, J = 1.8 Hz, 1H), 6.67 (d, J = 8.4 Hz, 1H), 6.52 (dd, J = 8.3, 1.9 Hz, 1H), 5.30 (s, 1H), 3.61 (s, 3H), 3.54 (s, 3H), 2.50–2.34 (m, 2H), 2.18 (d, J = 16.1 Hz, 1H), 1.99 (d, J = 15.9 Hz, 1H), 1.02 (s, 3H), 0.91 (s, 3H). ^{13}C NMR (101 MHz, DMSO-d_6) δ_{ppm} 192.8, 152.1, 147.9, 147.7, 146.5, 140.3, 136.2, 132.4, 128.7, 128.4, 127.9, 118.9, 111.7, 111.3, 107.6, 104.0, 55.3, 55.1, 50.4, 40.8, 34.5, 31.9, 29.0, 26.5.

Result and discussion

Nowadays, international researchers have attempted to elucidate important roles of the catalytic power of biologically enzymatic processes through hydrogen bonding via in vivo and in vitro.[43–57] In this regard, the design, synthesis, and application of the H-bond catalyst are our research interests. On the other hand, our experiences led us to develop pillar-layered metal–organic frameworks (MOFs) containing pending H-bond donor/acceptor functional groups. With this aim, we decided to synthesize TMU-17-UR as a new H-bond catalyst in the preparation of pyrazolo[3,4-b]quinolines as an important biological compound. The required starting materials were synthesized according to our recently reported educational synthetic organic theory.[58]

Catalyst preparation strategy

With the ever-increasing advances in science and technology, addressing environmental concerns should be prioritized. Efforts to preserve environmental resources have attracted the attention of researchers in recent years. As mentioned above, our research group has been working on the design and creation of various catalysts for catalytic and photocatalytic applications.[59–69] Here, the aim is to design and synthesize a new heterogeneous catalyst that will increase the range of existing catalysts. Accordingly, TMU-17-NH$_2$ was created as a pillar-layered MOF. In the following, through the post-modification method, urea groups were created on the desired framework. For this purpose, the NH$_2$ groups of the structure react with the isocyanate compound, and the urea group is created. In both stages, the solvothermal method has been used to create TMU-17-UR as an H-bond pillar-layered MOFs-based catalyst (Scheme 1).

The urea groups created on TMU-17-UR act as hydrogen bond donors/acceptors that activate the target bonds in the structure of the raw materials to perform the desired reaction. The proof of catalytic application of TMU-17-UR in the synthesis of pyrazolo[3,4-b]quinoline derivatives was investigated to reveal its performance. For this synthesis, raw materials synthesized with dimedone and various derivatives of aromatic aldehydes were used in a multicomponent reaction under solvent-free, mild, and green conditions. Purification of the products was done easily. Methods such as melting point, FT-IR, ^{1}H-NMR, and ^{13}C-NMR were used to prove the structure of the synthesized products (Scheme 2) (details are in ESI†).

Characterization

After the design and synthesis of the target catalyst, the chemical structure of TMU-17-UR was confirmed using FT-IR, XRD, SEM, BET/BJH, ^{13}C-NMR (See in ESI) and TGA/DTG techniques. The Fourier-transform infrared spectroscopy (FT-IR) was used to investigate the functional groups present in the initial and final catalyst structures. The results are comparatively shown in Fig. 2. The FT-IR spectrum of TMU-17-NH$_2$ is consistent with previous reports.[40] The peak of two branches, 3461 cm^{-1} and 3361 cm^{-1}, represents the NH$_2$ group. Also, the peak area of
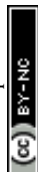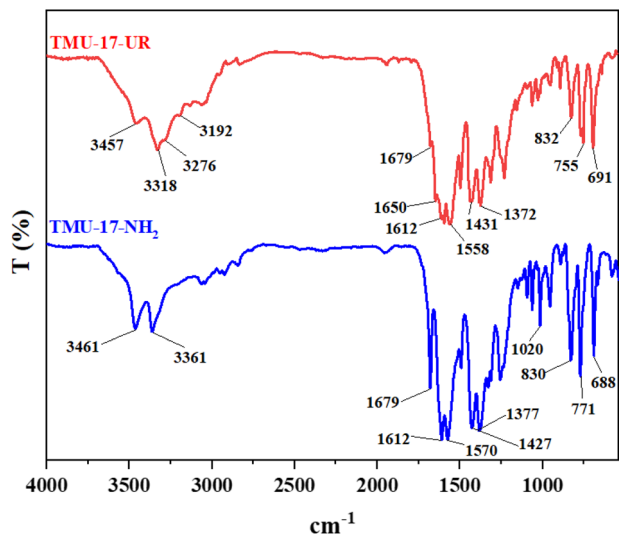
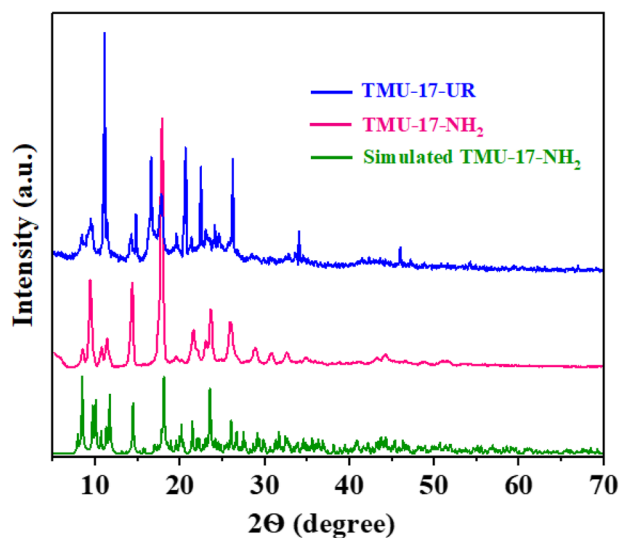Fig. 2 FT–IR spectrum of TMU-17-NH$_2$ and TMU-17-UR as an efficient H-bond pillar-layered MOFs-based catalyst.

Fig. 3 XRD spectra of simulated TMU-17-NH$_2$, TMU-17-NH$_2$ and TMU-17-UR as an efficient H-bond pillar-layered MOFs-based catalyst.

1679 cm^{-1} shows the presence of the carbonyl group in resonance, which is bonded with Zn metal. After the reaction of this structure with phenyl isocyanate, the urea group was created. The presence of peaks in the area of 3192–3457 cm^{-1} indicates the NH group in the urea moiety, and the peak in the area of 1650 cm^{-1} indicates its amidic carbonyl group in urea. The presence of these peaks in both structures indicates the formation of the desired structures (Fig. 2).

The XRD analysis is generally used to show the growth pattern of crystal plates. Metal–organic frameworks have a unique crystal pattern. Investigating the growth of crystalline

plates of structure TMU-17-NH$_2$ showed close agreement with the simulation previous reports.[40] After the post-modification method at the TMU-17-NH$_2$ by creating urea groups on it, the crystal structure has been preserved and remained stable (Fig. 3). In another study, the SEM technique was used to determine the morphology of the designed catalyst (Fig. S1, identification details are given in the ESI file†). SEM images of TMU-17-UR show uniform lumpy, and plate-like morphologies. This type of morphology may be effective in increasing its efficiency in the direction of the target catalytic application.

In another exploration, N$_2$ adsorption–desorption isotherms (BET) were used to investigate the surface area and pore size of TMU-17-UR as a hydrogen bonding catalyst (Fig. 4a). Based on the obtained results, the surface area based on the BET equation for TMU-17-UR was calculated at 75 m^2 g^{-1}. In addition, the total pore volume for TMU-17-UR was calculated to be 0.599 cm^3 g^{-1}. Also, the corresponding pores diameter distribution of the final catalyst is also shown in Fig. 4b. The mean pore diameter of the final catalyst is 31.7 nm. It should be noted that pillar-layered MOFs do not have a large surface area and pore size. Thus, the most previous reports did not have N$_2$ adsorption–desorption isotherms for this structure.[40,70]

One of the most important parameters and properties of catalysts that will be used in various organic reactions is their appropriate chemical and thermal stability. Thermogravimetry/derivative thermal gravimetric (TGA/DTG) and thermogravimetry/differential thermal analysis (TGA/DTA) analyses were used to prove the stability of the initial catalyst (TMU-17-NH$_2$) and its corresponding final catalyst (TMU-17-UR). The obtained results are shown in Fig. 5. The presented results show that TMU-17-UR has stability of up to 250 °C so that it can catalyze reactions up to this temperature. The reaction for the preparation of pyrazolo[3,4-*b*]quinoline derivatives in this report is at 100 °C. Due to the stability of this catalyst up to 250 °C, the proper stability of the catalyst is proven. Therefore, in the course of the desired reactions, the catalyst is not destroyed.

After the complete analysis of the synthesized catalyst and approving its structure, the use of TMU-17-UR as an efficient H-bond pillar-layered MOFs-based catalyst in the synthesis of pyrazolo[3,4-*b*]quinoline derivatives was evaluated. At first, the reaction conditions were optimized to determine the optimal synthesis conditions. For this purpose, the reaction between 3-(1*H*-indol-3-yl)-1*H*-pyrazol-5-amine (0.5 mmol, 0.099 g), 4-chlorobenzaldehyde (0.5 mmol, 0.07 g) and dimedone (0.5 mmol, 0.07 g), was chosen as the model reaction. First, solvent optimization was done, and the reaction was investigated in the presence of different organic solvents as well as solvent-free conditions (Fig. 6a). Solvent-free conditions were chosen as the best choice. Next, in the solvent-free conditions, the above reaction was carried out at different temperatures and with different amounts of catalyst. Based on the results obtained (Fig. 6b and c), performing the reaction at 100 °C and in the presence of 15 mg of TMU-17-UR yielded the best results.
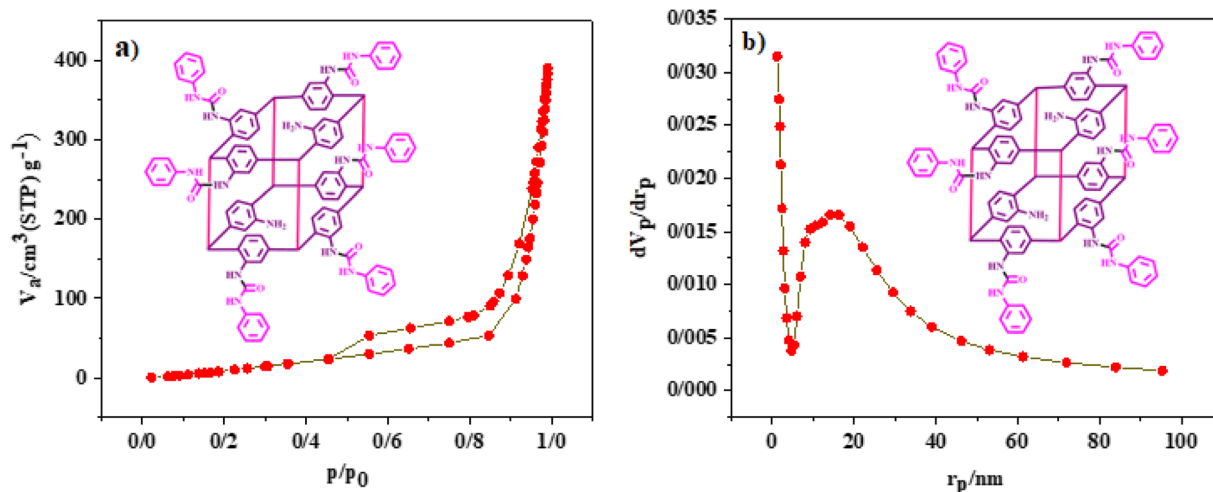
Fig. 4 (a) N_2 adsorption–desorption isotherms and (b) BJH plot TMU-17-UR as an efficient H-bond pillar-layered MOFs-based catalyst.
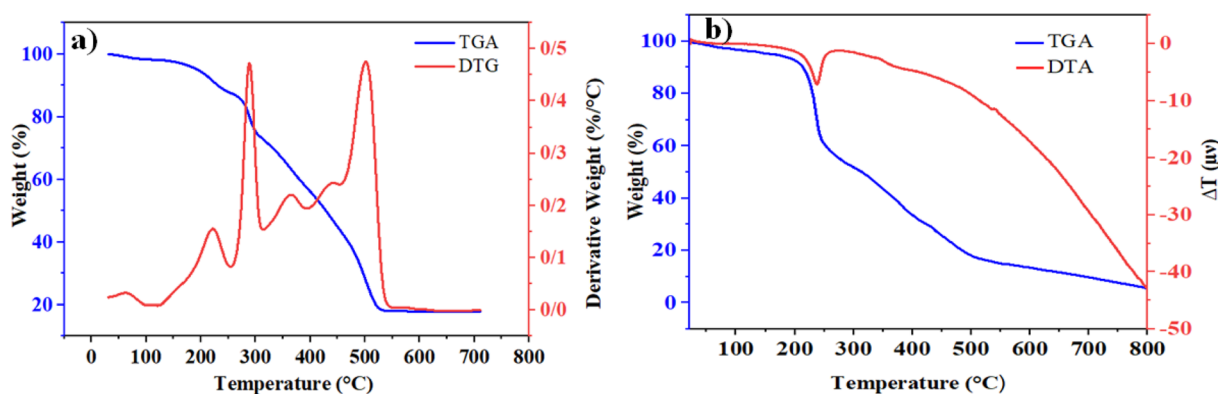

Fig. 5 (a) Thermogravimetry/derivative thermal gravimetric (TGA/DTG) analysis of TMU-17-NH$_2$ and (b) thermogravimetry/differential thermal analysis (TGA/DTA) analysis of TMU-17-UR as an efficient H-bond pillar-layered MOFs-based catalyst.

After determining the optimal reaction conditions (Fig. 6), a wide range of compounds pyrazolo[3,4-*b*]quinoline were synthesized with the help of the catalyst TMU-17-UR. As shown in Table 1, performing the model reaction in the presence of TMU-17-UR as an H-bond catalyst leads to the preparation of products in high yields (70–82%) and reduced reaction time (20–35 min). It should be noted that all the synthesized desired derivatives were fully identified, and their molecular structures were confirmed (identification details are given in the ESI file†).

To confirm how the synthesized products are formed, a proposed mechanism is presented in Scheme 3. According to the proposed mechanism, at first, the catalyst activates the dimedone carbonyl bond with its urea part, which acts as a hydrogen donor, and turns it into an enolic form. In a simultaneous process, the carbonyl aldehyde group is also activated by the catalyst and reacts with dimedone. From the condensation between these two, an intermediate (I) is created by removing one H$_2$O molecule. Next, 3-(1*H*-indol-3-yl)-1*H*-pyrazol-

5-amine or 3-(4-chlorophenyl)-1*H*-pyrazol-5-amine performs a nucleophilic attack on intermediate (I), and intermediate (II) is formed *via* a Michael addition reaction. Intermediate (II) undergoes tautomerization by the catalyst to form intermediate (III). In the next step, intermediate (III) undergoes catalytic intramolecular cyclization. Finally, by removing another H$_2$O molecule, the target product is created.[59,60]

Following the process of investigating the catalytic capabilities of TMU-17-UR as an efficient H-bond pillar-layered MOF-based catalyst, a comparative study was done on the synthesis of pyrazolo[3,4-*b*]quinolines using other catalysts. For this purpose, a wide range of organic and inorganic catalysts containing acidic, basic, and H-bond groups are used under the model reaction conditions. The results are shown in Table 2. According to the obtained results, the reaction in the presence of TMU-17-UR has better efficiency and a shorter reaction time in compared to other catalysts. One of the most important advantages of the presented heterogeneous catalysts is their recovery capability. Due to the heterogeneous nature of the

designed catalyst, its recyclability was also investigated. The results are shown in Fig. 7c. The results show that TMU-17-UR can be recycled and reused 5 times without much change in its catalytic activity. In order to check the stability of the recovered catalyst structure, FT-IR and XRD analyses were taken

from the recovered catalyst (Fig. 7a and b). The obtained results show that after recovery, the catalyst has good stability, and the above catalyst can be used and recycled several times without significant changes in the efficiency and reaction time.
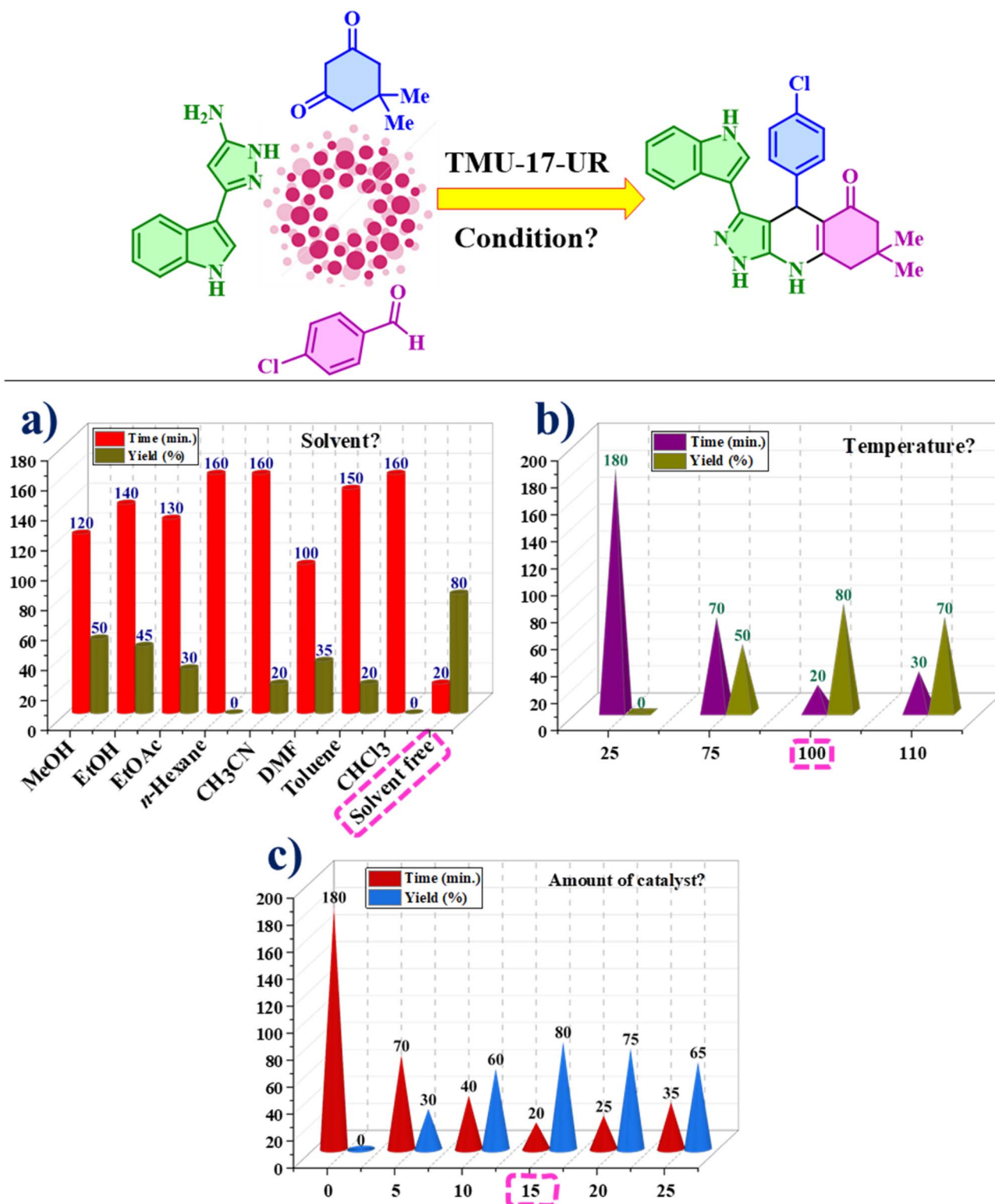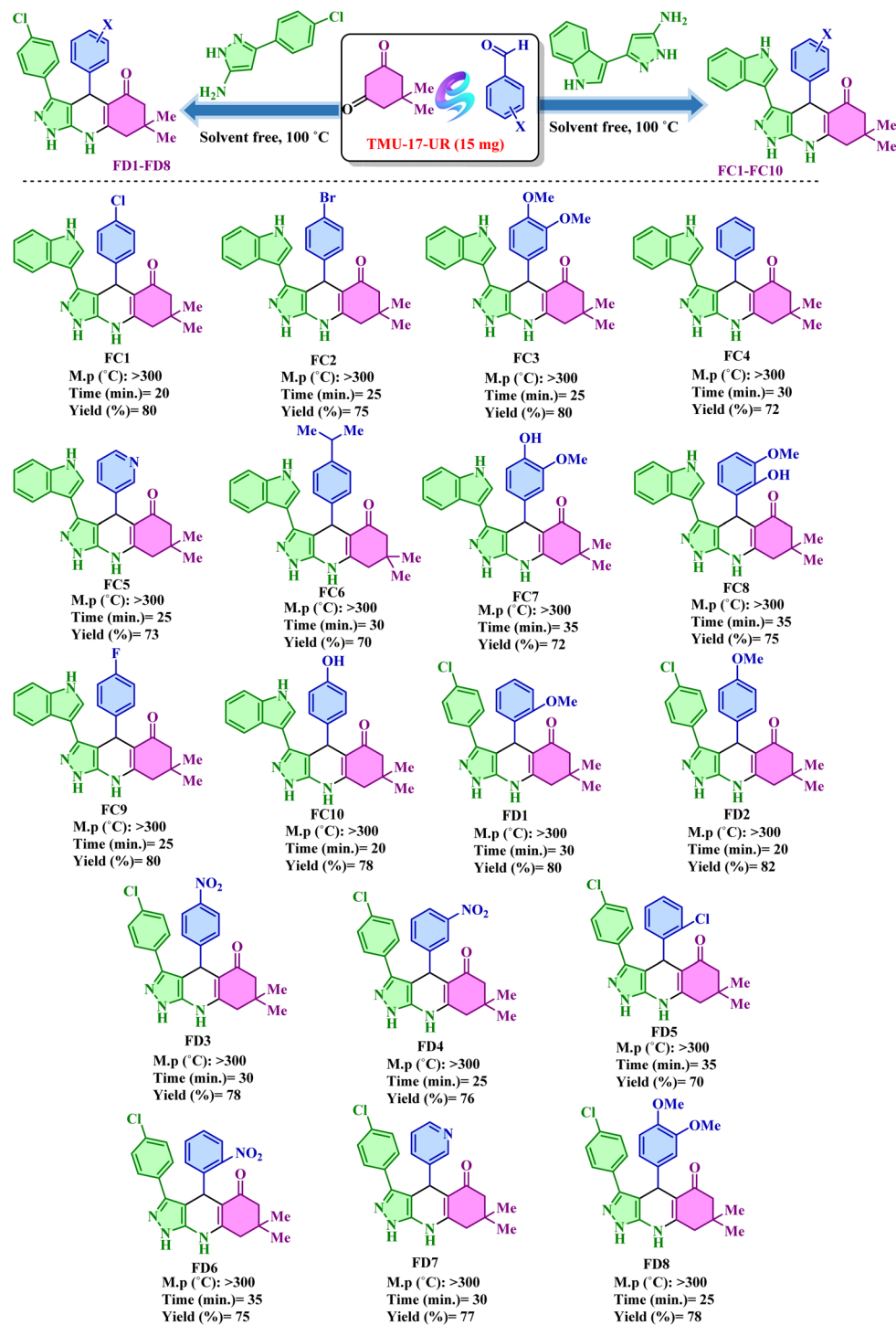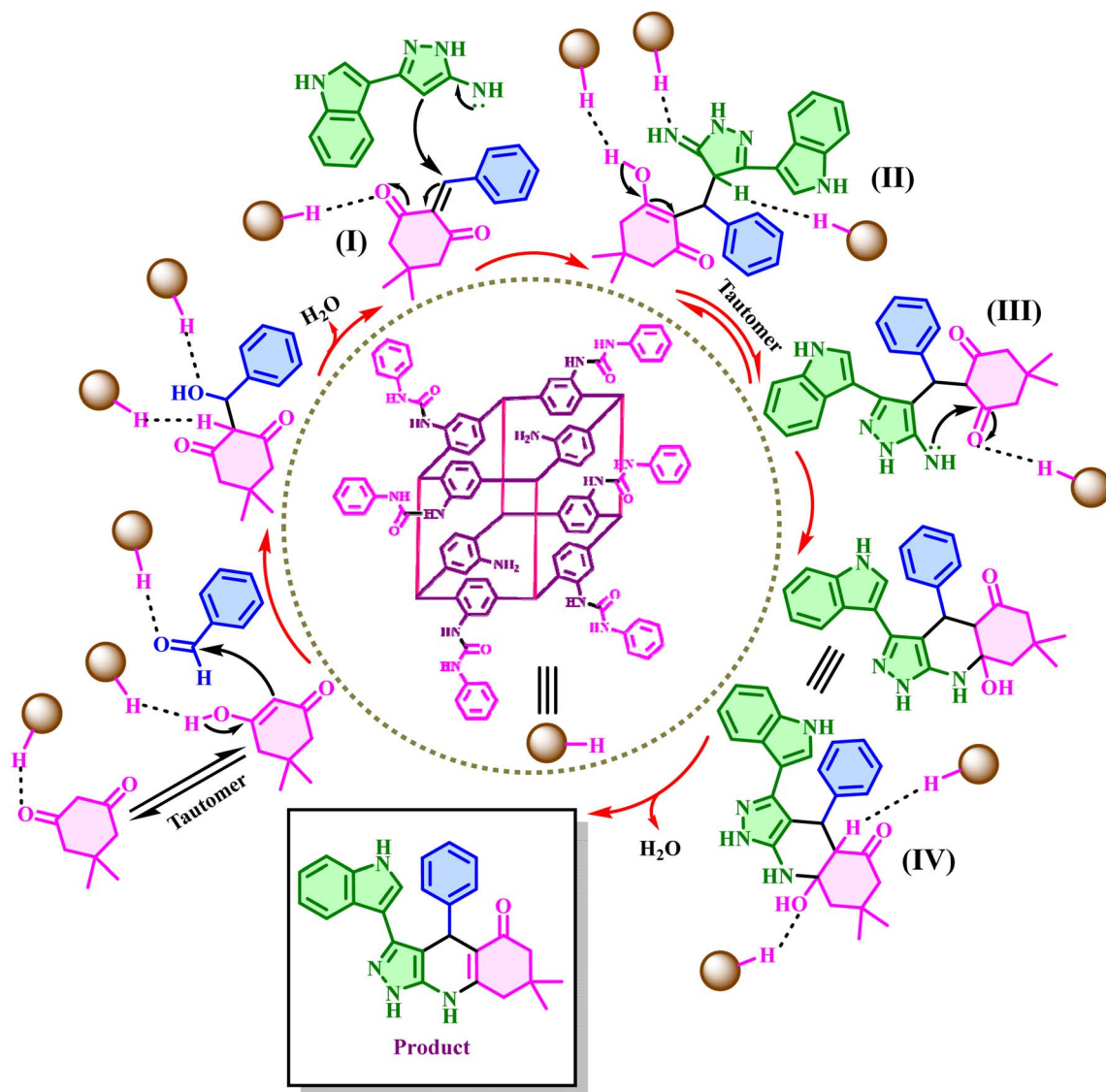

Fig. 6 Optimization of some model reaction parameters using TMU-17-UR as an efficient H-bond pillar-layered MOFs-based catalyst.

Table 1 The molecular structures of the desired synthesized pyrazolo[3,4-*b*]quinolines were obtained by using TMU-17-UR as an efficient H-bond pillar-layered MOF-based catalyst under solvent-free conditions

FC1
M.p (°C): >300
Time (min.)= 20
Yield (%)= 80

FC2
M.p (°C): >300
Time (min.)= 25
Yield (%)= 75

FC3
M.p (°C): >300
Time (min.)= 25
Yield (%)= 80

FC4
M.p (°C): >300
Time (min.)= 30
Yield (%)= 72

FC5
M.p (°C): >300
Time (min.)= 25
Yield (%)= 73

FC6
M.p (°C): >300
Time (min.)= 30
Yield (%)= 70

FC7
M.p (°C): >300
Time (min.)= 35
Yield (%)= 72

FC8
M.p (°C): >300
Time (min.)= 35
Yield (%)= 75

FC9
M.p (°C): >300
Time (min.)= 25
Yield (%)= 80

FC10
M.p (°C): >300
Time (min.)= 20
Yield (%)= 78

FD1
M.p (°C): >300
Time (min.)= 30
Yield (%)= 80

FD2
M.p (°C): >300
Time (min.)= 20
Yield (%)= 82

FD3
M.p (°C): >300
Time (min.)= 30
Yield (%)= 78

FD4
M.p (°C): >300
Time (min.)= 25
Yield (%)= 76

FD5
M.p (°C): >300
Time (min.)= 35
Yield (%)= 70

FD6
M.p (°C): >300
Time (min.)= 35
Yield (%)= 75

FD7
M.p (°C): >300
Time (min.)= 30
Yield (%)= 77

FD8
M.p (°C): >300
Time (min.)= 25
Yield (%)= 78

Scheme 3 The proposed mechanism for the synthesis of pyrazolo[3,4-*b*]quinolines using TMU-17-UR as an efficient H-bond pillar-layered MOFs-based catalyst.

Table 2 Synthesis of pyrazolo[3,4-*b*]quinoline derivatives in the presence of various catalysts

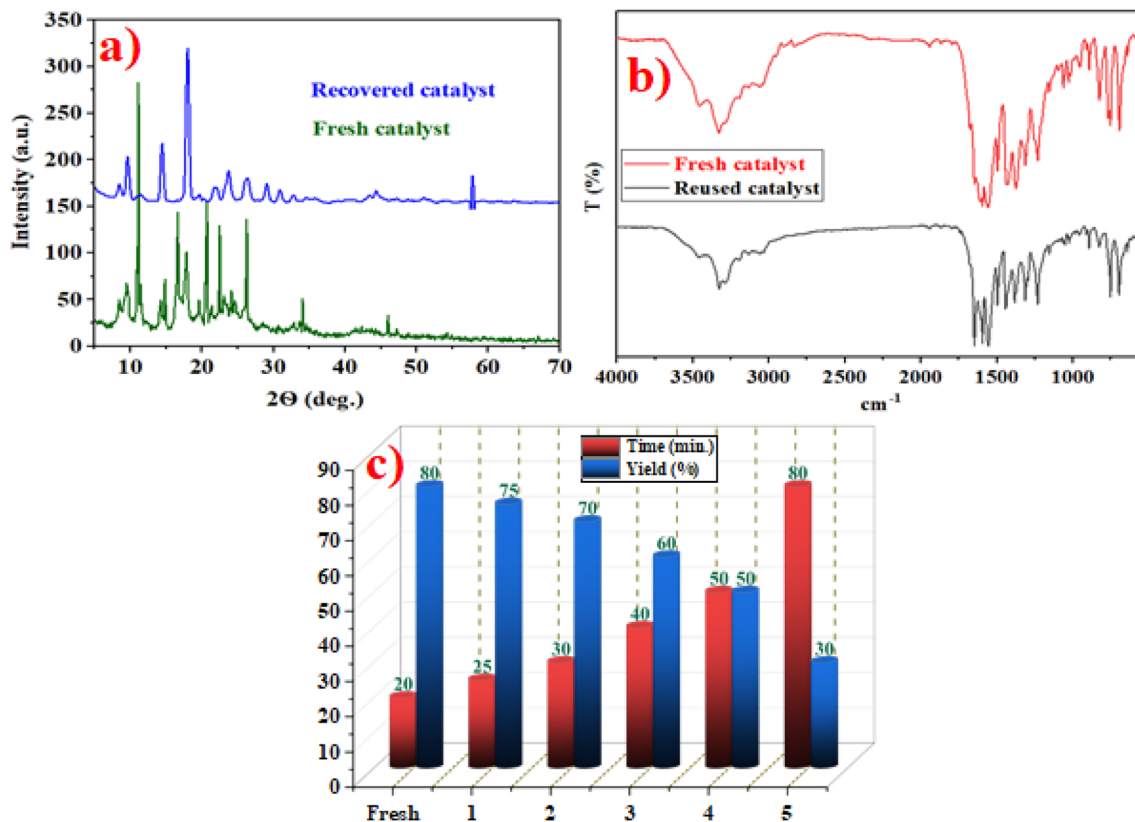| Entry	Catalyst	(Mol%)	Time (min)	Yield (%)
1	MIL-100(Cr)/NHEtN(CH$_2$PO$_3$H$_2$)$_2$ (ref. 71)	15 mg	75	35
2	GTBSA[72]	15 mg	6	65
3	*p*-TSA	15	120	40
4	NaOH	15	65	40
5	Pipyridine	15	180	30
6	[PVI-SO$_3$H]Cl[73]	15 mg	90	36
7	H$_2$SO$_4$	15	50	35
8	Et$_3$N	15	20	30
9	CQDs-N(CH$_2$PO$_3$H$_2$)$_2$/SBA-15 (ref. 74)	15 mg	50	45
10	CQDs-N(CH$_2$PO$_3$H$_2$)$_2$ (ref. 75)	15 mg	60	40
11	Ti-MOF-UR[24]	15 mg	45	50
12	SSA[76]	15 mg	80	25
13	TMU-17-NH$_2$ (ref. 40)	15 mg	60	40
14	**TMU-17-UR**	**15 mg**	**20**	**80**

Fig. 7 (a) XRD analysis, (b) FT–IR spectra and (c) recyclability of TMU-17-UR as an efficient H-bond pillar-layered MOFs-based catalyst in the synthesis of pyrazolo[3,4-b]quinoline derivatives.

Conclusion

The design and development of hydrogen bond catalysts occurred. In this regard, the TMU-17-UR catalyst was designed and synthesized as the target catalyst using a post-modification method to create urea fragments with hydrogen bond donors/acceptor's ability. The structure of the catalyst was evaluated to prove the correctness of its formation using various techniques. In the next step, the application of TMU-17-UR as an efficient H-bond pillar-layered MOFs-based catalyst in the preparation of a wide range of pyrazolo[3,4-b]quinoline derivatives was evaluated, and good results were obtained. Among the features of this work, we can mention performing the reaction under mild and green conditions, high speed of production of the desired products, high efficiency, and the ability to recycle and reuse the catalyst. The synthesis of a task-specific H-bond catalyst successfully occurred using suitable starting materials for creating urea moieties on the surface of the desired catalyst. The H-bond ability of the presented catalyst acts as an important factor in obtaining the desired results.

Data availability

The datasets used and/or analyzed during the current study available from the corresponding author on reasonable request.

Conflicts of interest

The authors declare no competing financial interest.

Acknowledgements

References

1 F. ZareKarizi, M. Joharian and A. Morsali, Pillar-layered MOFs: functionality, interpenetration, flexibility and applications, *J. Mater. Chem. A*, 2018, **6**, 19288–19329.

2 Z. H. Xuan, D. S. Zhang, Z. Chang, T. L. Hu and X. H. Bu, Targeted structure modulation of "pillar-layered" metal-organic frameworks for CO_2 capture, *Inorg. Chem.*, 2014, **53**, 8985–8990.

3 X. J. Hong, Q. Wei, Y. P. Cai, B. B. Wu, H. X. Feng, Y. Yu and R. F. Dong, Pillar-layered metal-organic framework with sieving effect and pore space partition for effective separation of mixed gas C_2H_2/C_2H_4, *ACS Appl. Mater. Interfaces*, 2017, **9**, 29374–29379.

4 D. C. Mayer, J. K. Zaręba, G. Raudaschl-Sieber, A. Pöthig, M. Chołuj, R. Zaleśny, M. Samoć and R. A. Fischer,

Postsynthetic framework contraction enhances the two-photon absorption properties of pillar-layered metal-organic frameworks, *Chem. Mater.*, 2020, **32**, 5682–5690.

5 Z. Zhu, Z. Wang, Q. H. Li, Z. Ma, F. Wang and J. Zhang, Porphyrin metal-organic frameworks with bilayer and pillar-layered frameworks and third-order nonlinear optical properties, *Dalton Trans.*, 2023, **52**, 4309–4314.

6 T. Yan, J. Yang, J. Lu, L. Zhou, Y. Zhang and G. He, Facile Synthesis of Ultra-microporous Pillar-Layered Metal-Organic Framework Membranes for Highly H$_2$-Selective Separation, *ACS Appl. Mater. Interfaces*, 2023, **15**, 20571–20582.

7 Y. Meng, Y. Du, Y. Lin, Y. Su, R. Li, Y. Feng and S. Meng, A two-fold interpenetration pillar-layered metal-organic frameworks based on BODIPY for chemo-photodynamic therapy, *Dyes Pigm.*, 2021, **188**, 109174.

8 X. Zhang, Y. Z. Zhang, Y. Q. Jin, L. Geng, D. S. Zhang, H. Hu, T. Li, B. Vang and J. R. Li, Pillar-layered metal-organic frameworks based on a hexaprismane [Co6(μ3-OH)6] cluster: structural modulation and catalytic performance in aerobic oxidation reaction, *Inorg. Chem.*, 2020, **59**, 11728–11735.

9 I. Senkovska, V. Bon, L. Abylgazina, M. Mendt, J. Berger, G. Kieslich, P. Petkov, J. L. Fiorio, J. Joswig, T. Heine, L. Schaper, C. Bachetzky, R. Schmid, R. A. Fischer, A. Pöppl, E. Brunner and S. Kaskel, Understanding MOF flexibility: An analysis focused on pillared layer MOFs as a model system, *Angew. Chem., Int. Ed.*, 2023, **62**, e202218076.

10 V. J. Lillo, J. Mansilla and J. M. Saa, Organocatalysis by networks of cooperative hydrogen bonds: Enantioselective direct Mannich addition to preformed arylideneureas, *Angew. Chem.*, 2016, **128**, 4384–4388.

11 M. Singh and S. Neogi, Urea-engineering mediated hydrogen-bond donating Friedel-Crafts alkylation of indoles and nitroalkenes in a dual-functionalized microporous metal-organic framework with high recyclability and pore-fitting-induced size-selectivity, *Inorg. Chem. Front.*, 2022, **9**, 1897–1911.

12 Y. L. Liu and J. Zhou, Catalytic Asymmetric Strecker Reaction: Bifunctional Chiral Tertiary Amine/Hydrogen-Bond Donor Catalysis Joins the Field, *Synthesis*, 2015, **47**, 1210–1226.

13 Q. Wang, X. Yao, S. Tang, X. Lu, X. Zhang and S. Zhang, Urea as an efficient and reusable catalyst for the glycolysis of poly(ethylene terephthalate) wastes and the role of hydrogen bond in this process, *Green Chem.*, 2012, **14**, 2559–2566.

14 M. Liu, J. Wu and H. Hou, Metal-Organic Framework (MOF)-based materials as heterogeneous catalysts for C-H bond activation, *Chem.–Eur. J.*, 2019, **25**, 2935–2948.

15 C. M. McGuirk, M. J. Katz, C. L. Stern, A. A. Sarjeant, J. T. Hupp, O. K. Farha and C. A. Mirkin, Turning on catalysis: incorporation of a hydrogen-bond-donating squaramide moiety into a Zr metal-organic framework, *J. Am. Chem. Soc.*, 2015, **137**, 919–925.

16 M. Y. Zhao, J. N. Zhu, P. Li, W. Li, T. Cai, F. F. Cheng and W. W. Xiong, Structural variation of transition metal-organic frameworks using deep eutectic solvents with different hydrogen bond donors, *Dalton Trans.*, 2019, **48**, 10199–10209.

17 A. Dhakshinamoorthy, A. M. Asiri and H. Garcia, Formation of C-C and C-heteroatom bonds by C-H activation by metal organic frameworks as catalysts or supports, *ACS Catal.*, 2018, **9**, 1081–1102.

18 W. Gong, Y. Liu, H. Li and Y. Cui, Metal-organic frameworks as solid Brønsted acid catalysts for advanced organic transformations, *Coord. Chem. Rev.*, 2020, **420**, 213400.

19 (a) G. Cai, P. Yan, L. Zhang, H. C. Zhou and H. L. Jiang, Metal-organic framework-based hierarchically porous materials: synthesis and applications, *Chem. Rev.*, 2021, **121**, 12278–12326; (b) H. Sepehrmansourie, M. Mohammadi Rasooll, M. Zarei, M. A. Zolfigol and Y. Gu, Application of metal-organic frameworks with sulfonic acid tags in the synthesis of pyrazolo[3,4-b] pyridines via a cooperative vinylogous anomeric-based oxidation, *Inorg. Chem.*, 2023, **62**, 9217–9229.

20 Y. Yao, X. Zhao, G. Chang, X. Yang and B. Chen, Hierarchically porous metal-organic frameworks: synthetic strategies and applications, *Small Struct.*, 2023, **4**, 2200187.

21 A. Karmakar, S. Hazra and A. J. Pombeiro, Urea and thiourea based coordination polymers and metal-organic frameworks: Synthesis, structure and applications, *Coord. Chem. Rev.*, 2022, **453**, 214314.

22 J. M. Roberts, B. M. Fini, A. A. Sarjeant, O. K. Farha, J. T. Hupp and K. A. Scheidt, Urea metal-organic frameworks as effective and size-selective hydrogen-bond catalysts, *J. Am. Chem. Soc.*, 2012, **134**, 3334–3337.

23 J. Y. Song and S. H. Jhung, Adsorption of pharmaceuticals and personal care products over metal-organic frameworks functionalized with hydroxyl groups: quantitative analyses of H-bonding in adsorption, *Chem. Eng. J.*, 2017, **322**, 366–374.

24 Z. Torkashvand, H. Sepehrmansourie, M. A. Zolfigol and M. A. As' Habi, Application of Ti-MOF-UR as a new porous catalyst for the preparation of pyrazolo[3,4-b]quinoline and pyrazolo[4,3-e]pyridines, *Mol. Catal.*, 2023, **541**, 113107.

25 R. B. Lin, Y. He, P. Li, H. Wang, W. Zhou and B. Chen, Multifunctional porous hydrogen-bonded organic framework materials, *Chem. Soc. Rev.*, 2019, **48**, 1362–1389.

26 A. Dhakshinamoorthy, A. M. Asiri and H. Garcia, Formation of C-C and C-heteroatom bonds by C-H activation by metal organic frameworks as catalysts or supports, *ACS Catal.*, 2018, **9**, 1081–1102.

27 A. Weyesa and E. Mulugeta, Recent advances in the synthesis of biologically and pharmaceutically active quinoline and its analogues: a review, *RSC Adv.*, 2020, **10**, 20784–20793.

28 Z. X. Niu, Y. T. Wang, S. N. Zhang, Y. Li, X. B. Chen, S. Q. Wang and H. M. Liu, Application and synthesis of thiazole ring in clinically approved drugs, *Eur. J. Med. Chem.*, 2023, **250**, 115172.

29 A. Mermer, T. Keles and Y. Sirin, Recent studies of nitrogen containing heterocyclic compounds as novel antiviral agents: A review, *Bioorg. Chem.*, 2021, **114**, 105076.

30 R. F. Costa, L. C. Turones, K. V. N. Cavalcante, I. A. Rosa Júnior, C. H. Xavier, L. P. Rosseto, H. B. Napolitano, P. F. S. Castro, M. L. F. Neto, G. M. Galvão, R. Menegatti, G. R. Pedrino, E. A. Costa, J. L. R. Martins and J. O. Fajemiroye, Heterocyclic compounds: pharmacology of pyrazole analogs from rational structural considerations, *Front. Pharmacol.*, 2021, **12**, 666725.

31 M. A. El-Bindary and A. A. El-Bindary, Synthesis, characterization, DNA binding, and biological action of dimedone arylhydrazone chelates, *Appl. Organomet. Chem.*, 2022, **36**, e6576.

32 F. A. Mohamed, A. El-Megied, A. Saadia and R. Mohareb, Synthesis and application of novel reactive dyes based on Dimedone moiety, *Egypt. J. Chem.*, 2020, **63**, 4447–4455.

33 M. C. Ríos and J. Portilla, Recent advances in synthesis and properties of pyrazoles, *Chemistry*, 2022, **4**, 940–968.

34 M. Marinescu, Synthesis of antimicrobial benzimidazole-pyrazole compounds and their biological activities, *Antibiotics*, 2021, **10**, 1002.

35 K. Husain, E. A. M. Saleh and I. Hassan, Synthesis, Antibacterial, and Antifungal Evaluation of New Class of Pyrimido[4,5-*d*]pyrimidine, Pyrazolo[3,4-*d*]pyrimidine, and Pyrimido[4,5-*b*]quinoline Derived from α, α-Ketene Dithioacetals as fused Five and Six-membered Heterocycle Derivatives, *Russ. J. Bioorg. Chem.*, 2023, **49**, 1367–1380.

36 M. R. Toosi, M. Pordel and M. R. Bozorgmehr, Synthesis of Heterocyclic Systems 3*H*-furo [2,3-*b*]imidazo[4,5-*f*]quinolines and 3*H*-furo[2,3-*b*]pyrazolo[4,3-*f*]quinolines as New Antibacterial Agents, *Pharm. Chem. J.*, 2022, **56**, 206–214.

37 A. Danel, E. Gondek, M. Kucharek, P. Szlachcic and A. Gut, 1*H*-Pyrazolo[3,4-*b*]quinolines: Synthesis and Properties over 100 Years of Research, *Molecules*, 2022, **27**, 2775.

38 N. R. Babu, R. S. Raju, R. R. Alavala, N. Malothu and Y. Padmavathi, Design, Synthesis, Anti-Tubercular Evaluation and Teratogenicity Studies of Furanyl Pyrazolo [3,4-*b*]Quinoline-5-Ones, *Russ. J. Bioorg. Chem.*, 2023, **49**, 127–138.

39 M. Mroueh, W. H. Faour, W. N. Shebaby, C. F. Daher, T. M. Ibrahim and H. M. Ragab, Synthesis, biological evaluation and modeling of hybrids from tetrahydro-1*H*-pyrazolo[3,4-*b*]quinolines as dual cholinestase and COX-2 inhibitors, *Bioorg. Chem.*, 2020, **100**, 103895.

40 (*a*) V. Safarifard, S. Beheshti and A. Morsali, An interpenetrating amine-functionalized metal-organic framework as an efficient and reusable catalyst for the selective synthesis of tetrahydro-chromenes, *CrystEngComm*, 2015, **17**, 1680–1685; (*b*) M. Yadollahi, H. Hamadi and V. Nobakht, Capture of iodine in solution and vapor phases by newly synthesized and characterized encapsulated Cu_2O nanoparticles into the TMU-17-NH_2 MOF, *J. Hazard. Mater.*, 2020, **399**, 122872.

41 A. El-Mekabaty, H. A. Etman and A. Mosbah, Synthesis of some new fused pyrazole derivatives bearing indole moiety as antioxidant agents, *J. Heterocycl. Chem.*, 2016, **53**, 894–900.

42 T. Takahashi, A. Sakuraba, T. Hirohashi, T. Shibata, M. Hirose, Y. Haga, K. Nonoshita, T. Kanno, J. Ito, H. Iwaasa, A. Kanatani, T. Fukami and N. Sato, Novel potent neuropeptide Y Y5 receptor antagonists: Synthesis and structure-activity relationships of phenylpiperazine derivatives, *Bioorg. Med. Chem.*, 2006, **14**, 7501–7511.

43 P. R. Schreiner and A. Wittkopp, H-bonding additives act like Lewis acid catalysts, *Org. Lett.*, 2002, **4**, 217–220.

44 C. X. Yan, F. Yang, X. Yang, D. G. Zhou and P. P. Zhou, Insights into the diels-alder reaction between 3-vinylindoles and methyleneindolinone without and with the assistance of hydrogen-bonding catalyst bisthiourea: Mechanism, origin of stereoselectivity, and role of catalyst, *J. Org. Chem.*, 2017, **82**, 3046–3061.

45 S. Shirakawa, S. Liu, S. Kaneko, Y. Kumatabara, A. Fukuda, Y. Omagari and K. Maruoka, Tetraalkylammonium salts as hydrogen-bonding catalysts, *Angew. Chem., Int. Ed.*, 2015, **54**, 15767–15770.

46 F. Secci, M. Arca, A. Frongia and P. P. Piras, Tetrazole amides as hydrogen-bonding donor catalysts in the chemoselective oxidation of sulphides and disulphides, *Catal. Sci. Technol.*, 2014, **4**, 1407–1415.

47 S. Meninno, A. Vidal-Albalat and A. Lattanzi, Asymmetric epoxidation of alkylidenemalononitriles: key step for one-pot approach to enantioenriched 3-substituted piperazin-2-ones, *Org. Lett.*, 2015, **17**, 4348–4351.

48 B. W. Gruijters, M. A. Broeren, F. L. van Delft, R. P. Sijbesma, P. H. Hermkens and F. P. Rutjes, Catalyst recycling via hydrogen-bonding-based affinity tags, *Org. Lett.*, 2006, **8**, 3163–3166.

49 J. W. Park, J. H. Park and C. H. Jun, Dual functionalities of hydrogen-bonding self-assembled catalysts in chelation-assisted hydroacylation, *J. Org. Chem.*, 2008, **73**, 5598–5601.

50 S. Kaneko, Y. Kumatabara, S. Shimizu, K. Maruoka and S. Shirakawa, Hydrogen-bonding catalysis of sulfonium salts, *Chem. Commun.*, 2016, **53**, 119–122.

51 P. C. Rao and S. Mandal, Friedel-Crafts Alkylation of Indoles with Nitroalkenes through Hydrogen-Bond-Donating Metal-Organic Framework, *ChemCatChem*, 2017, **9**, 1172–1176.

52 X. Zhao, J. J. Gong, K. Yuan, F. Sha and X. Y. Wu, Highly enantioselective intramolecular Rauhut-Currier reaction catalyzed by chiral thiourea-phosphine, *Tetrahedron Lett.*, 2015, **56**, 2526–2528.

53 Y. Lin, M. Cai, Z. Fang and H. Zhao, A highly efficient heterogeneous copper-catalyzed Chan-Lam coupling between thiols and arylboronic acids leading to diaryl sulfides under mild conditions, *Tetrahedron*, 2016, **72**, 3335–3343.

54 J. P. Byrne, S. Blasco, A. B. Aletti, G. Hessman and T. Gunnlaugsson, Formation of self-templated 2,6-bis(1,2,3-triazol-4-yl)pyridine[2]catenanes by triazolyl hydrogen bonding: selective anion hosts for phosphate, *Angew. Chem., Int. Ed.*, 2016, **55**, 8938–8943.

55 M. S. Taylor and E. N. Jacobsen, Asymmetric catalysis by chiral hydrogen-bond donors, *Angew. Chem., Int. Ed.*, 2006, **45**, 1520–1543.

56 P. R. Schreiner, Metal-free organocatalysis through explicit hydrogen bonding interactions, *Chem. Soc. Rev.*, 2003, **32**, 289–296.

57 A. G. Doyle and E. N. Jacobsen, Small-molecule H-bond donors in asymmetric catalysis, *Chem. Rev.*, 2007, **107**, 5713–5743.

58 M. A. Zolfigol, S. Azizian, M. Torabi, M. Yarie and B. Notash, The importance of non-stoichiometric ratio of reactants in organic synthesis, *J. Chem. Educ.*, 2024, **101**, 877–881.

59 M. Mohammadi Rasooll, H. Sepehrmansourie, M. Zarei, M. A. Zolfigol, M. Hosseinifard and Y. Gu, Catalytic Application of Functionalized Bimetallic-Organic Frameworks with Phosphorous Acid Tags in the Synthesis of Pyrazolo[4,3-e]pyridines, *ACS Omega*, 2023, **8**, 25303–25315.

60 (a) M. M. Rasooll, H. Sepehrmansourie, M. A. Zolfigol, M. Hosseinifard, S. L. Hosseini and Y. Gu, Application of a new porous bimetallic H-bond catalyst in the preparation of biological henna-based pyrazolo[3,4-b]quinolines via a cooperative vinylogous anomeric based oxidation, *Mol. Catal.*, 2025, **570**, 114628; (b) M. M. Rasooll, Magnetic metal-organic frameworks (MMOFs): As multipurpose catalysts, *Iran. J. Catal.*, 2025, **15**, 152512.

61 H. Sepehrmansourie, H. Alamgholiloo, M. A. Zolfigol, N. N. Pesyan and M. M. Rasooll, Nanoarchitecting a Dual Z-Scheme Zr-MOF/Ti-MOF/g-C$_3$N$_4$ Heterojunction for Boosting Gomberg-Buchmann-Hey Reactions under Visible Light Conditions, *ACS Sustain. Chem. Eng.*, 2023, **11**, 3182–3193.

62 (a) F. Jalili, H. Sepehrmansourie, M. Zarei, M. A. Zolfigol, A. Khazaei and M. A. As' Habi, Application of novel metal-organic frameworks containing sulfonic acid pendings in synthesis of chromeno[4,3-d]pyrimidines via back to back anomeric based oxidation, *Arabian J. Chem.*, 2024, **17**, 105635; (b) A. R. Ataee-Najari, M. M. Rasooll, M. Zarei, M. A. Zolfigol, A. Ghorbani-Choghamarani and M. Hosseinifard, Catalytic application of a bimetallic-organic framework with phosphorus acid groups in the preparation of pyrido[2,3-d]pyrimidines via cooperative vinylogous anomeric-based oxidation, *RSC Adv.*, 2025, **15**, 10150–10163.

63 M. M. Rasooll, H. Ahmadi, H. Sepehrmansourie, M. A. Zolfigol, E. Ghytasranjbar and A. Mohammadzadeh, Synthesis and application of a bimetallic-MOFs with sulfonic acid tags in preparation of biologically active nicotinonitriles via cooperative vinylogous anomeric-based oxidation, *RSC Adv.*, 2025, **15**, 4636–4651.

64 H. Sepehrmansourie, H. Alamgholiloo, N. N. Pesyan and M. A. Zolfigol, A MOF-on-MOF strategy to construct double Z-scheme heterojunction for high-performance photocatalytic degradation, *Appl. Catal., B*, 2023, **321**, 122082.

65 S. Babaee, H. Sepehrmansourie, M. Zarei, M. A. Zolfigol and M. Hosseinifard, Synthesis of picolinates via a cooperative vinylogous anomeric-based oxidation using UiO-66(Zr)-N(CH$_2$PO$_3$H$_2$)$_2$ as a catalyst, *RSC Adv.*, 2023, **13**, 22503–22511.

66 H. Sepehrmansourie, M. Zarei, M. A. Zolfigol, S. Babaee, S. Azizian and S. Rostamnia, Catalytic synthesis of new pyrazolo[3,4-b]pyridine via a cooperative vinylogous anomeric-based oxidation, *Sci. Rep.*, 2022, **12**, 14145.

67 B. Danishyar, H. Sepehrmansourie, H. Ahmadi, M. Zarei, M. A. Zolfigol and M. Hosseinifard, Application of Nanomagnetic Metal-Organic Frameworks in the Green Synthesis of Nicotinonitriles via Cooperative Vinylogous Anomeric-Based Oxidation, *ACS Omega*, 2023, **21**, 18479–18490.

68 N. Zarei, M. Yarie, M. Torabi and M. A. Zolfigol, Urea-rich porous organic polymer as a hydrogen bond catalyst for Knoevenagel condensation reaction and synthesis of 2,3-dihydroquinazolin-4(1H)-ones, *RSC Adv.*, 2024, **14**, 1094–1105.

69 M. Bayatani, M. Torabi, M. Yarie, M. A. Zolfigol and Z. Farajzadeh, Fabrication of an imidazolium-based magnetic ionic porous organic polymer for efficient heterogeneous catalysis of Betti reaction, *J. Mol. Liq.*, 2023, **390**, 122863.

70 A. Mirzaie, T. Musabeygi and A. Afzalinia, Sonochemical synthesis of magnetic responsive Fe$_3$O$_4$@TMU-17-NH$_2$ composite as sorbent for highly efficient ultrasonic-assisted denitrogenation of fossil fuel, *Ultrason. Sonochem.*, 2017, **38**, 664–671.

71 H. Sepehrmansouri, M. Zarei, M. A. Zolfigol, A. R. Moosavi-Zare, S. Rostamnia and S. Moradi, Multilinker phosphorous acid anchored En/MIL-100(Cr) as a novel nanoporous catalyst for the synthesis of new N-heterocyclic pyrimido[4,5-b]quinolines, *Mol. Catal.*, 2020, **481**, 110303.

72 M. Zarei, H. Sepehrmansourie, M. A. Zolfigol, R. Karamian and S. H. M. Farida, Novel nano-size and crab-like biological-based glycoluril with sulfonic acid tags as a reusable catalyst: Its application to the synthesis of new mono-and bis-spiropyrans and their in vitro biological studies, *New J. Chem.*, 2018, **42**, 14308–14317.

73 H. Sepehrmansourie, M. Zarei, R. Taghavi and M. A. Zolfigol, Mesoporous ionically tagged cross-linked poly (vinyl imidazole) s as novel and reusable catalysts for the preparation of N-heterocycle spiropyrans, *ACS Omega*, 2019, **4**, 17379–17392.

74 M. M. Rasooll, H. Sepehrmansourie, M. Zarei, M. A. Zolfigol and S. Rostamnia, Phosphonic acid tagged carbon quantum dots encapsulated in SBA-15 as a novel catalyst for the preparation of N-heterocycles with pyrazolo, barbituric acid and indole moieties, *Sci. Rep.*, 2022, **12**, 20812.

75 M. M. Rasooll, M. Zarei, M. A. Zolfigol, H. Sepehrmansourie, A. Omidi, M. Hasani and Y. Gu, Novel nano-architectured carbon quantum dots (CQDs) with phosphorous acid tags as an efficient catalyst for the synthesis of multisubstituted 4H-pyran with indole moieties under mild conditions, *RSC Adv.*, 2021, **11**, 25995–26007.

76 M. A. Zolfigol, Silica sulfuric acid/NaNO$_2$ as a novel heterogeneous system for production of thionitrites and disulfides under mild conditions, *Tetrahedron*, 2001, **57**, 9509–9511.